Planta (2022) 255:44
https://doi.org/10.1007/s00425-022-03823-4

ORIGINAL ARTICLE

Minc03328 effector gene downregulation severely affects *Meloidogyne incognita* parasitism in transgenic *Arabidopsis thaliana*

Valdeir Junio Vaz Moreira[1,2,3] · Isabela Tristan Lourenço-Tessutti[1,4] · Marcos Fernando Basso[1,4] · Maria Eugênia Lisei-de-Sa[1,3,5] · Carolina Vianna Morgante[1,4,6] · Bruno Paes-de-Melo[1,7] · Fabrício Barbosa Monteiro Arraes[1,2,4] · Diogo Martins-de-Sa[1,3] · Maria Cristina Mattar Silva[1,4] · Janice de Almeida Engler[4,8] · Maria Fatima Grossi-de-Sa[1,4,9]

Received: 30 October 2021 / Accepted: 4 January 2022 / Published online: 20 January 2022

Abstract

Main conclusion ***Minc03328*** **effector gene downregulation triggered by** ***in planta*** **RNAi strategy strongly reduced plant susceptibility to** ***Meloidogyne incognita*** **and suggests that** ***Minc03328*** **gene is a promising target for the development of genetically engineered crops to improve plant tolerance to** ***M. incognita*****.**

Abstract *Meloidogyne incognita* is the most economically important species of root-knot nematodes (RKN) and causes severe damage to crops worldwide. *M. incognita* secretes several effector proteins to suppress the host plant defense response, and manipulate the plant cell cycle and other plant processes facilitating its parasitism. Different secreted effector proteins have already been identified in *M. incognita*, but not all have been characterized or have had the confirmation of their involvement in nematode parasitism in their host plants. Herein, we characterized the *Minc03328* (*Minc3s00020g01299*) effector gene, confirmed its higher expression in the early stages of *M. incognita* parasitism in plants, as well as the accumulation of the Minc03328 effector protein in subventral glands and its secretion. We also discuss the potential for simultaneous downregulation of its paralogue *Minc3s00083g03984* gene. Using the *in planta* RNA interference strategy, *Arabidopsis thaliana* plants overexpressing double-stranded RNA (dsRNA) were generated to specifically targeting and downregulating the *Minc03328* gene during nematode parasitism. Transgenic Minc03328-dsRNA lines that significantly downregulated *Minc03328* gene expression during *M. incognita* parasitism were significantly less susceptible. The number of galls, egg masses, and [galls/egg masses] ratio were reduced in these transgenic lines by up to 85%, 90%, and 87%, respectively. Transgenic Minc03328-dsRNA lines showed the presence of fewer and smaller galls, indicating that parasitism was hindered. Overall, data herein strongly suggest that Minc03328 effector protein is important for *M. incognita* parasitism establishment. As well, the *in planta* Minc03328-dsRNA strategy demonstrated high biotechnological potential for developing crop species that could efficiently control RKN in the field.

Keywords Crop protection · Effector protein · *In planta* RNAi · New biotechnological tools · Plant–nematode interaction · Root-knot nematode

Abbreviations

DAI Days after inoculation
eGFP Enhanced green fluorescent protein
pJ2 Parasitic second-stage juvenile
ppJ2 Pre-parasitic second-stage juvenile
RKN Root-knot nematode

Introduction

Plant–parasitic nematodes (PPNs) are one of the major agricultural pathogens in several crops, causing annually significant economic losses worldwide (Bernard et al. 2017). Among them, root-knot nematodes (RKN) comprises several obligate sedentary endoparasites from the genus

Communicated by Dorothea Bartels.

✉ Maria Fatima Grossi-de-Sa
fatima.grossi@embrapa.br

Extended author information available on the last page of the article

Meloidogyne spp. (Trudgill and Blok 2001). *Meloidogyne incognita* is the most reported species infecting several economically important crops such as cotton, eggplant, and soybean (Abad et al. 2008). Its life cycle consists of the following stages: egg, ppJ2 (pre-parasitic second-stage juveniles), pJ2 (parasitic second-stage juveniles), J3, and J4 non-feeding juveniles, and females. The pJ2, J3, and J4 parasitic stages, and females are typically sedentary endophytes, while eggs and ppJ2 are exophytes (Triantaphyllou and Hirschmann 1960; Castagnone-Sereno et al. 2013). During a compatible interaction, RKNs disrupt root cells by hyper activating their cell cycle, increasing the parasitized cells size called giant-feeding cells, causing surrounding vascular cell hyperproliferation, forming feeding sites within root swellings named-galls (Engler et al. 2012; Shukla et al. 2018). Consequently, these nematode-infected roots are disrupted on water, and nutrient uptake and, consequently, plants reduced growth and yield (Melakeberhan et al. 1987; Carneiro et al. 2002; Lu et al. 2014).

For successful parasitism, *M. incognita* secrete a cocktail of effector proteins that act in *trans* to manipulate different biological processes and defense responses of the host plants (Nguyen et al. 2018; Grossi-de-Sa et al. 2019; Zhao et al. 2019). Genome data mining and secretome analyses from *M. incognita* pJ2s allowed the identification of several candidate effector proteins (Huang et al. 2003; Bellafiore et al. 2008; Rutter et al. 2014). For example, Bournaud et al. (2018) showed that the MiPM effector protein interacts with the soybean CSN5 subunit of the COP9 signalosome protein to facilitate *M. incognita* penetration and parasitism in host plants. Mendes et al. (2021b) reported that MiEFF1/Minc17998 effector protein interacts with soybean GmHub6 protein to promote *M. incognita* parasitism in host plants. Truong et al. (2021) demonstrated that the MiEFF1 effector protein also interacts with *Arabidopsis thaliana* cytosolic glyceraldehyde-3-phosphate dehydrogenase proteins promoting *M. incognita* parasitism in plants. Mendes et al. (2021a) verified that the Minc00344 and Mj-NULG1a effector proteins interact with GmHub10 protein to promote the *M. incognita* and *M. javanica* parasitism in soybean. Interestingly, the downregulation of the *Minc01696*, *Minc00344*, or *Minc00801* effector genes using *in planta* RNAi (RNAi, host induced gene silencing) strategy in stable transgenic tobacco and soybean hairy roots strongly disturbed *M. incognita* parasitism (unpublished data). Rutter et al. (2014) revealed that the *Minc03328* effector gene expression was significantly upregulated during *M. incognita* parasitism in plants, ranging from 3 to 14 days after inoculation (DAI), followed by a strong post-transcriptional regulation at 21 DAI. In addition, Rutter et al. (2014) also indicated that *Minc03328* effector transcript specifically accumulated into *M. incognita* subventral glands (SvG) of pJ2 and J3 stages. Despite this interesting preliminary information, the importance of the Minc03328 effector protein for successful parasitism of *M. incognita* in host plants has been not yet further investigated.

Herein, we applied *in planta* RNAi strategy for the production of double-stranded RNA (dsRNA) to target and downregulate *Minc03328* effector transcripts in *M. incognita* during plant parasitism. We then evaluated the importance of this effector for *M. incognita* parasitism in these transgenic plants. Stable transgenic *A. thaliana* lines, overexpressing a dsRNA capable of producing siRNAs molecules targeting and posttranscriptionally regulating *Minc03328* gene were successfully generated, and the susceptibility level of these transgenic Minc03328-dsRNA lines to *M. incognita* was assessed. Morphological analyzes illustrated that downregulation of *Minc03328* affected nematode as well as gall morphology, and immunocytochemical analysis localized Minc03328 protein in the nematode SvG and its secretion *in planta*. Thus, the importance of the Minc03328 effector protein in the *M. incognita versus* host plant interaction and its potential biotechnological use via *in planta* RNAi strategy in economically important crops are herein discussed.

Materials and methods

Sequence features

Minc03328 effector gene, its paralogue *Minc3s00083g03984* gene, and their orthologous genes were retrieved from BioProject ID PRJEB8714 (sample: ERS1696677) (Blanc-Mathieu et al. 2017) from WormBase Parasite Database version WBPS13 (Lee et al. 2017). Subsequently, conserved domains were identified using CDD Database from NCBI (Marchler-Bauer et al. 2015), PFAM Database from EMBL-EBI (El-Gebali et al. 2018), and InterPro Scan (Blum et al. 2020), while nuclear export signal (NES) was predicted with cutoff 0.5 using NetNES 1.1 Server (la Cour et al. 2004), and nuclear localization signal (NLS) was predicted with cutoff 0.5 using NLStradamus online tool (Nguyen Ba et al. 2009). The secretory proteins were predicted using MatureP tool (http://www.stepdb.eu/MatureP.php) (Orfanoudaki et al. 2017). For inferring potential orthologous and paralogous genes corresponding to each effector studied here, comparative genomic trees were generated from BioProject PRJEB8714 (Blanc-Mathieu et al. 2017) by the WormBase ParaSite Database using the Ensembl Compara tools implemented in this database (Vilella et al. 2009) and using default parameters.

Minc03328 in silico expression level

The expression levels of the *Minc03328* effector gene and its paralogue *Minc3s00083g03984* gene in different *M.*

incognita life stages were determined using transcriptome datasets from BioProject number: PRJNA390559 (Choi et al. 2017) retrieved of the BioSample database (NCBI). Particularly, 15 transcriptome libraries from *M. incognita* egg, J2, pJ2/J3, J4, and female stages were generated by Choi et al. (2017) using Truseq RNA Sample Prep Kit (Illumina), and mRNAs were paired-end sequenced (2 × 101 nucleotides) using Illumina HiSeq 2000 technology. The raw data (fastq files) were downloaded from NCBI using the following accession numbers: egg stage: SRR5684407, SRR5684403, and SRR5684417; J2 stage: SRR5684416, SRR5684412, and SRR5684414; pJ2/J3 stage: SRR5684413, SRR5684415, and SRR5684404; J4 stage: SRR5684408, SRR5684406, and SRR5684405; and female stage: SRR5684410, SRR5684409, and SRR5684411. Fastq files were trimmed using Trimmomatic version 0.39 (Bolger et al. 2014). The quantification was performed by the Kallisto program version 0.43.0 (Bray et al. 2016) using a genome reference retrieved from WormBase Parasite Database (BioProject ID PRJEB8714) (Szitenberg et al. 2017). The target gene expression in different nematode life stages was estimated as transcript per million (TPM) by the Kallisto program.

Histopathological analysis of *Nicotiana tabacum* roots infected with *M. incognita*

N. tabacum var. SR1 Petit Havana plants were inoculated with 1.000 *M. incognita* ppJ2 and maintained under greenhouse conditions. Infected root tips were harvested during nematode parasitism at 0, 5, 10, 15, and 22 DAI, washed in water, slightly dried with a paper towel, and stained with acid fuchsin, according to Bybd et al. (1983). Then, root samples were immersed in 2.5% (*v/v*) sodium hypochlorite solution for clarification and washed with water for 10 min. Finally, roots were completely immersed in acid fuchsin solution (1.25 g acid fuchsin solubilized in 1:3 v/v glacial acetic acid and distilled water). For improved root staining, samples were gently heated in a microwave for 1 min. After staining, acid fuchsin solution was discarded, and roots were rinsed and transferred to acidified glycerol solution (24:1 glycerol and hydrochloric acid, v/v). Histopathological analyses were performed by bright-field microscopy and images were generated by a Zeiss AxioCam MR.

Minc03328 expression profile during *M. incognita* parasitism in *N. tabacum*

Total RNA was extracted using Quick-RNA™ Plant Miniprep kit (Zymo Research, Irvine, CA, USA) from *M. incognita* eggs, ppJ2, and infected *N. tabacum* galls at 5, 10, 15, and 22 DAI. The RNA concentration was estimated using a spectrophotometer (NanoDrop 2000, Thermo Scientific, Waltham, MA, USA), and integrity was evaluated with 1% agarose gel electrophoresis. RNA samples were treated with RNase-free RQ1 DNase I (Promega, Madison, WI, USA), according to the manufacturer's instructions. DNase-treated RNA was used as template for cDNA synthesis using Oligo-$(dT)_{20}$ primer (100 µM), random hexamers (50 µM), and SuperScript III RT (Life Technologies, Carlsbad, CA, USA), according to the manufacturer's instructions. After synthesis, cDNA samples were diluted at 1:10 with nuclease-free water. RT-qPCR assays were performed in Applied Biosystems 7500 Fast Real-Time PCR System (Applied Biosystems, Foster City, CA, USA) using 2 µl cDNA, 0.2 µM gene-specific primer (Suppl. Table S1), and GoTaq® qPCR Master Mix (Promega, Madison,WI, USA). Gene expression level was normalized using *Mi18S* and *MiGAPDH* as endogenous reference genes. Three biological replicates were used for each treatment, composed of four plants that totaled at least 50 galls. All cDNA samples were carried out in technical triplicate, while primer efficiencies were previously determined and target-specific amplification was confirmed by a single and distinct peak in the melting curve analysis. The relative expression level was calculated using 2^-ΔCT method (Schmittgen and Livak 2008). The data were subjected by variance analysis (ANOVA) and, when significant, means were compared using Tukey test at 5% significance level using SASM-Agri statistical package (Canteri et al. 2001).

Minc03328 effector protein immunolocalization in *M. incognita*

M. incognita-infected galls at 1, 5, and 10 DAI from wild-type *A. thaliana* plants and uninfected roots were collected and fixed in 4% (v/v) formaldehyde in 50 mM PIPES buffer pH 6.9 (Sigma-Aldrich, St. Louis, MO, USA). Then, these galls were dehydrated and embedded in butyl methylmethacrylate essentially as described by Kronenberger et al. (1993) and Vieira et al. (2012). A primary anti-Minc03328 polyclonal antibody was produced in rabbits by GenScript (Leiden, The Netherlands) for use in this study, where a short amino acid sequence (14 aa length) with low sequence identity to other *M. incognita* or plant proteins was selected (Suppl. File S1). The anti-Minc03328 antibody and a commercial secondary antibody goat anti-rabbit IgG conjugated with Alexa 488 (Molecular Probes, Eugene, OR, USA) were diluted 20- and 300-fold, respectively, in blocking solution (1% w/v bovine serum albumin in 50 mM PIPES buffer pH 6.9 (Sigma-Aldrich, St. Louis, MO, USA), and 0.2% v/v DMSO). As a negative control, the primary antibody was omitted in some slides. Galls sections (5 µm) were incubated for 30 min in acetone, and adhered tissues were rehydrated in decreasing absolute ethanol concentrations. Slides were then washed twice for 15 min in PIPES buffer pH 6.9 (Sigma-Aldrich) and blocked with blocking buffer (2% w/v bovine

serum albumin in PIPES buffer, pH 6.9) for 3 h incubating at room temperature. Sections were then incubated overnight with primary antibody at 4 °C and then 1 h at 37 °C. Next, a 2 h incubation at 37 °C was performed with a secondary antibody. DNA was stained with 1 µg/mL 4',6-diamidino-2-phenylindole (Sigma-Aldrich) in water. Finally, slides were quickly washed in distilled water to remove salts and gently coverslipped in 90% (*v*/*v*) glycerol for observation under an Axioplan (Zeiss, Jena, Germany) equipped for epifluorescence microscopy. Images were acquired with an Axiocam digital camera (Zeiss).

Agrobacterium-mediated genetic transformation of *A. thaliana* to generate Minc03328-dsRNA lines

The binary vector (named GS62658-4 virMinc03328) was synthesized and assembled by Epoch Life Science (Missouri, TX, USA), and subsequently transfected into *A. tumefaciens* strain GV3101. A 200 bp fragment from *Minc03328* encoding sequence was chosen as dsRNA template to activate *in planta* RNAi strategy (Suppl. Table S2). BLASTp and BLASTn analyses from NCBI and WormBase databases were performed to evaluate sequence similarity to other metazoans and *A. thaliana* genes to minimize off-target silencing. Then, this 200 bp fragment was cloned in sense and antisense strands separated by the *pdk intron* and under control of constitutive *pUceS8.3* promoter (Grossi-de-Sa et al. 2013) (Fig. 2a). The *hptII* gene (hygromycin resistance) was used as a selection marker gene under control of the *pUbi3* promoter, while enhanced *green fluorescent protein* (*eGFP*) gene was used as molecular marker protein in transgenic Minc03328-dsRNA lines (Fig. 2a). The *A. thaliana* ecotype Col-0 inflorescences were genetically transformed by the floral dip method (Clough and Bent 1998). Then, seeds from *A. thaliana* lines were screened in vitro using 15 mg/L hygromycin B (Invitrogen, Carlsbad, CA, USA) according to Harrison et al. (2006). Subsequently, hygromycin-resistant plants were acclimated in pots containing commercial substrate and maintained in a growth room (22 °C, 70–75% relative humidity, and ~ 100 µmol photons m^{-2} s^{-1} light intensity with a 16/8 h photoperiod). Acclimated plants were screened by PCR using specific primers targeting *eGFP* gene (Suppl. Table S1) and GoTaq® DNA Polymerase mix (Promega, Madison, WI, USA). Total DNA was purified from *A. thaliana* leaves according to Doyle and Doyle method (1987). Amplicons were analyzed in 1% agarose gel electrophoresis stained with ethidium bromide. In addition, GFP protein accumulation in transgenic lines was confirmed under a Zeiss inverted LSM510 META laser scanning microscope using 488-nm excitation line and 500–530-nm band-pass filter (Zeiss). Finally, several independent transgenic lines were generated, T_1-to-T_3 generations were advanced, and four homozygous T_3 transgenic Minc03328-dsRNA lines were selected for bioassays with *M. incognita* race 3.

Minc03328-dsRNA transgenic plants' inoculation and susceptibility assessment

M. incognita ppJ2 race 3 were obtained from tomato plants (*Solanum lycopersicum* cv. Santa Clara) inoculated and maintained for 2 or 3 months under greenhouse conditions (25–37 °C, 12–16 h light, ~ 70% humidity). The infected 60–90-day-old roots were washed and ground using a blender after treatment with 0.5% sodium hypochlorite. Eggs were harvested, rinsed with tap water, and subsequently separated from root debris using 100–550 µm sieves (Hussey and Barker 1973). The eggs were then hatched under aerobic conditions incubating at 28 °C, and ppJ2 were harvested every 2 days, gently decanted at 4 °C, and quantified under a microscope using counting chambers. *A. thaliana* plants from four transgenic Minc03328-dsRNA lines ($n = 5$–20 plants) additional to wild-type control plants were inoculated with 500 M. *incognita* ppJ2 race 3 suspended in distilled water. Plant susceptibility level to *M. incognita* was evaluated at 60 DAI measuring number of galls per plant, number of egg masses per plant and, then, calculating [galls/egg masses number] ratio. Then, data were subjected to ANOVA analysis, and when significant, means were compared by the Tukey test at 5% significance level using SASM-Agri statistical package (Canteri et al. 2001).

The transgene expression and *Minc03328* gene downregulation

Total RNA was extracted from transgenic and wild-type galls at 5 DAI using TRIzol (Life Technologies, Carlsbad, CA, USA), according to the manufacturer's recommendations. The transgene expression in transgenic *A. thaliana* lines was confirmed by RT-qPCR analysis using specific primers to target *pdk intron* sequence. The relative expression values of the transgene were normalized using *AtActin 2*, *AtGAPDH*, and *AtEF1* as reference endogenous genes (Suppl. Table S1). In another hand, *Minc03328* gene downregulation in *M. incognita* during its parasitism in transgenic *A. thaliana* lines was confirmed by RT-qPCR analysis using *MiGAPDH*, *MiActin,* and *Miβ-tubulin* as reference endogenous genes (Suppl. Table S1). All Ct values were corrected according to primer's efficiencies using the Miner tool (http://www.miner.ewindup.info), and relative gene expression was calculated using 2^-ΔCT method (Schmittgen and Livak 2008) as described above. Normalized expression data obtained from *A. thaliana* and *M. incognita* reference genes were generated using geNorm software (St-Pierre et al. 2017) with *M-values* assigned between 0.4 and 0.7. Each

treatment was composed of three biological replicates, while each biological replicate included three plants. All samples were evaluated in technical triplicates.

Gall morphology analysis of Minc03328-dsRNA transgenic *A. thaliana*

The *M. incognita*-induced galls in *A. thaliana* transgenic line #1 and wild-type control plants were excised from 45 DAI plants and fixed in 2% (*v*/*v*) glutaraldehyde in 50 mM PIPES buffer pH 6.9 (Sigma-Aldrich) for 1 week. Fixed galls were then dehydrated using an ethanol gradient (10, 30, 50, 70, 90, and 100%; *v*/*v*) and embedded in Technovit 7100 resin (Kulzer, Friedrichsdorf, Germany), according to the manufacturer's recommendations. Then, galls sections (5 µm) were stained in 0.05% (*w*/*v*) toluidine blue in 100 mM sodium phosphate buffer (pH 5.5) and rinsed in distilled water. Slides were mounted with Depex (Sigma-Aldrich, St. Louis, MO, USA). Stained sections were observed under bright-field light microscopy, and images were obtained with a digital AxioCamHRc camera for morphological analyses (Carl Zeiss, Oberkochen, Germany). At least 20 galls were analyzed for gall and nematode morphology observations.

Results

In silico sequence analysis of *Minc03328* effector gene

The *Minc03328* (ID: *Minc3s00020g01299*) gene sequence has 2.06 kb length organized in 6 exons and 5 intron sequences, flanked by 5′- and 3′-UTR sequences. Its CDS sequence has 1428 nucleotides length, encoding a 475 amino acid protein with a predicted 6.67 isoelectric point and 54.99 kDa molecular weight (Table 1; Suppl. Table S2). In addition, two start codons were identified in the 5'-UTR or beginning of CDS 5' region. Blanc-Mathieu et al. (2017) have suggested that *Minc03328* translation starts from this second start codon (Suppl. Table S2). The Minc03328 effector protein has a predicted non-cytoplasmatic domain, nuclear exportation signal, nuclear localization signal, secretory signal peptide located in the N-terminal (amino acids at + 1 to + 22 position), and absence of an internal transmembrane domain (Table 1; Suppl. Table S2). The absence of a transmembrane domain and presence of a secretion signal peptide suggest as features needed to address Minc03328 effector protein to vesicles in the exocytic-secretory pathway and subsequent secretion of the mature protein during *M. incognita* parasitism in plants.

The comparative genomic tree generated from *Minc03328* gene showed that the *Minc3s00083g03984* gene can be consistently considered as its paralogue gene, while *scf7180000417668.g1585* (*M. floridensis*), *tig00000829.g51954* (*M. arenaria*), *scaffold1253_cov168.g2771* (*M. javanica*), *NXFT01001574.1.4100_g* (*M. graminicola*), and *scaffold8370_cov173.g11786* (*M. enterolobii*) can be considered as their orthologous genes in other *Meloidogyne* species (Suppl. Fig. S1). Pairwise comparisons of nucleotide sequences showed that *Minc03328* effector gene has 50–70% identity with other effector genes present in *Meloidogyne* sp. (Suppl. Fig. S2), whereas it has 60–99% identity with its paralogue and orthologous genes (Fig. 1a). A phylogenetic tree generated from nucleotide sequences showed that *Minc03328* effector gene is more closely related to *tig00000829.g51954* (*M. arenaria*) and *scf7180000417668.g1585* (*M. floridensis*) genes (Fig. 1b). All these collective data from in silico sequence analysis suggest that the *Minc03328* effector gene is distant at the sequence and phylogenetic levels from other *Meloidogyne* effector genes, but has remarkable characteristics closely associated with *M. incognita* parasitism in plants.

Minc03328 gene expression and protein immunolocalization in *M. incognita*

From transcriptome data mining, it was possible to identify *Minc03328* gene expression profile, as well as its paralogue *Minc3s00083g03984* gene, in different *M. incognita* life stages (egg, pJ2, ppJ2/J3, J4, and female) during nematode parasitism in plants (Fig. 1c). The highest expression level of these two genes was observed in the pJ2/J3 stage followed by the J4 stage, which coincides with onset of the *M. incognita* parasitism in plants (Fig. 1c). These in silico gene expression data were confirmed by real-time RT-qPCR analysis. The RT-qPCR analysis indicated that *Minc03328* gene is overexpressed during *M. incognita* parasitism in *N. tabacum* specifically at 5 DAI, confirming its expression modulation at the beginning of the parasitic process and suggesting its specific association during the plant–nematode interaction (Fig. 1d and e). In accordance, fuchsin-stained *N. tabacum* roots showed that *M. incognita* pJ2s at 5 DAI are fully established in infected roots, while at 10 and 15 DAI was verified that *M. incognita* J3 and J3/J4 induced successful feeding sites, and progressively developed into females at 22 DAI (Fig. 1d). Subsequently, the Minc03328 effector protein was immunolocalized and showed to accumulate in subventral glands during *M. incognita* parasitism in *N. tabacum* at 5 to 10 DAI (Fig. 1f). Punctually localized green fluorescence was observed close to the nematode head and strongly suggested *in planta* secretion of the Minc03328 effector protein during early *M. incognita* parasitism. It is expected that this signal to be very weak and localized, since this is one (or two) proteins embedded in a cocktail of a number of other nematode secreted molecules. Particularly, a significant fluorescence signal was also observed in some giant cells near

Table 1 Features of the *Minc03328* effector gene, its paralogue *Minc3s00083g03984* gene, and their orthologous genes in other *Meloidogyne* sp.

Gene	Gene ID	Gene description	Nucleotide (bp)	Amino acid	Expression	Immunolocalization	CDD domain	PFAM domain	NES motif	NLS motif	Secretory protein
M. incognita	*Minc3s00020g01299 Minc03328*	Effector involved in nematode parasitism	1428	475	3, 7, and 14 DAI/pJ2 to J4	Subventral gland cells	No	Non-cytoplasmatic domain	Yes	Yes	Yes
M. incognita	*Minc3s00083g03984*	Paralogue gene of the *Minc03328*	1452	482	pJ2 to J4	Undefined	No	Non-cytoplasmatic domain	Yes	No	Yes
M. floridensis	*scf7180000417668.g1585*	Orthologue gene of the *Minc03328*	531	176	Undefined	Undefined	No	Non-cytoplasmatic domain	No	No	Yes
M. floridensis	*scf7180000418513.g2509*	Orthologue gene of the *Minc03328*	1296	431	Undefined	Undefined	no	Non-cytoplasmatic domain	Yes	Yes	Yes
M. arenaria	*tig00000829.g51954*	Orthologue gene of the *Minc03328*	1458	485	Undefined	Undefined	No	Non-cytoplasmatic domain	Yes	Yes	Yes
M. arenaria	*tig00003009.g30158*	Orthologue gene of the *Minc03328*	1425	474	Undefined	Undefined	No	Non-cytoplasmatic domain	Yes	Yes	Yes
M. arenaria	*tig00000677.g45944*	Orthologue gene of the *Minc03328*	1470	489	Undefined	Undefined	No	Non-cytoplasmatic domain	Yes	No	Yes
M. javanica	*scaffold1170_cov195.g2611*	Orthologue gene of the *Minc03328*	1227	408	Undefined	Undefined	No	Non-cytoplasmatic domain	Yes	No	Yes
M. javanica	*scaffold1253_cov168.g2771*	Orthologue gene of the *Minc03328*	1227	408	Undefined	Undefined	No	Non-cytoplasmatic domain	Yes	No	Yes
M. graminicola	*NXFT01001574.1.4100_g*	Orthologue gene of the *Minc03328*	1347	448	Undefined	Undefined	No	Non-cytoplasmatic domain	No	Yes	Yes
M. enterolobii	*scaffold8370_cov173.g11786*	Orthologue gene of the *Minc03328*	1476	491	Undefined	Undefined	No	Non-cytoplasmatic domain	Yes	Yes	Yes
M. enterolobii	*scaffold23549_cov323.g21895*	Orthologue gene of the *Minc03328*	1175	391	Undefined	Undefined	DUF4954	cl28804	Yes	Yes	
M. enterolobii	*scaffold41831_cov389.g26027*	Orthologue gene of the *Minc03328*	333	110	Undefined	Undefined	No	Non-cytoplasmatic domain	Yes	No	Yes

Table 1 (continued)

Gene	Gene ID	Gene description	Nucleotide (bp)	Amino acid	Expression	Immunolocalization	CDD domain	PFAM domain	NES motif	NLS motif	Secretory protein
M. incognita	*Minc3s00036g02098* *Minc01696**	Effector involved in nematode parasitism	2020	573	3 dpi/J2	Subventral gland cells	smart00220 cl31127	Pkinase (CL0016)	Yes	No	Yes

The gene sequences were retrieved of BioProject PRJEB8714 (2017) from WormBase database version WBPS14 (Lee et al. 2017)

DUF4954 or cl28804 domain of unknown function; *smart00220* serine/threonine protein kinases, catalytic domain; *CL0016* protein kinase superfamily

*Outgroup used in the sequence analysis

the head tip of nematode (Fig. 1g, letters i and ii), while in some galls, a strong fluorescence signal was observed along the cell wall suggesting the presence of Minc03328 protein, but we cannot totally exclude that eventual unspecific staining from remaining sticking antibody in some tissue might occur (Fig. 1g, letters iii). No fluorescence signal was observed in late J2/J3/J4 stages ranging from 15 to 22 DAI (Fig. 1h, letters i and ii). In addition, absence of the fluorescence signal also was observed in females and egg masses at 22 to 45 DAI (Fig. 1i, letter i and ii), but interestingly, some punctual fluorescence signals were visualized within eggs possibly already containing ppJ2 that will hatch (Fig. 1i, letter ii and iii). Thus, these data collectively showed that *Minc03328* effector gene is expressed in infective juveniles (pJ2 and J3 stages) and during early stages of *M. incognita* parasitism in plants (5 DAI). As well, that the encoded effector protein accumulates in subventral glands of ppJ2 and pJ2, is visibly secreted and might be present in giant cells, suggesting that this effector may be involved in promoting *M. incognita* parasitism in plants.

Plant genetic transformation and susceptibility level assessment

A 200 bp length fragment was selected from *Minc03328* effector gene to apply the *in planta* RNAi strategy (Suppl. Table S2). It is plausible to consider that the RNAi strategy generated for *Minc03328* gene downregulation may have also downregulated the *Minc3s00083g03984* paralogue gene due to high sequence identity (Suppl. File S2). In addition, this 200-bp sequence from *Minc03328* effector gene used did not show any significant hits in the *A. thaliana* transcriptome after pairwise sequence comparison, indicating a reduced probability of potential off-target effects in these transgenic plants. The 200-bp DNA fragment was cloned into sense and antisense orientation separated by the *pdk intron,* while its expression was triggered by the constitutive *pUceS8.3* promoter (Fig. 2a). To provide more evidence that the Minc03328 effector protein is directly linked to *M. incognita* parasitism in plants, we successfully generated 12 stable transgenic *A. thaliana* lines using *A. tumefaciens*-mediated delivery system (floral dip). Transgenic Minc03328-dsRNA lines were systematically screened in vitro under hygromycin selection (Suppl. Fig. S3). After advancing to T_3 generation, four transgenic lines (Line #1 to #4) were selected to compare their susceptibility level to *M. incognita* with wild-type control plants. PCR analyses using specific primers targeting *eGFP* gene confirmed transgene insertion in all transgenic lines (Fig. 2b). Transgene expression was checked in all transgenic Minc03328-dsRNA lines by detecting the GFP fluorescent protein accumulation through confocal microscopy (Fig. 2c). Next, 15–20 plants from each transgenic line and wild-type control plants were individually transferred to

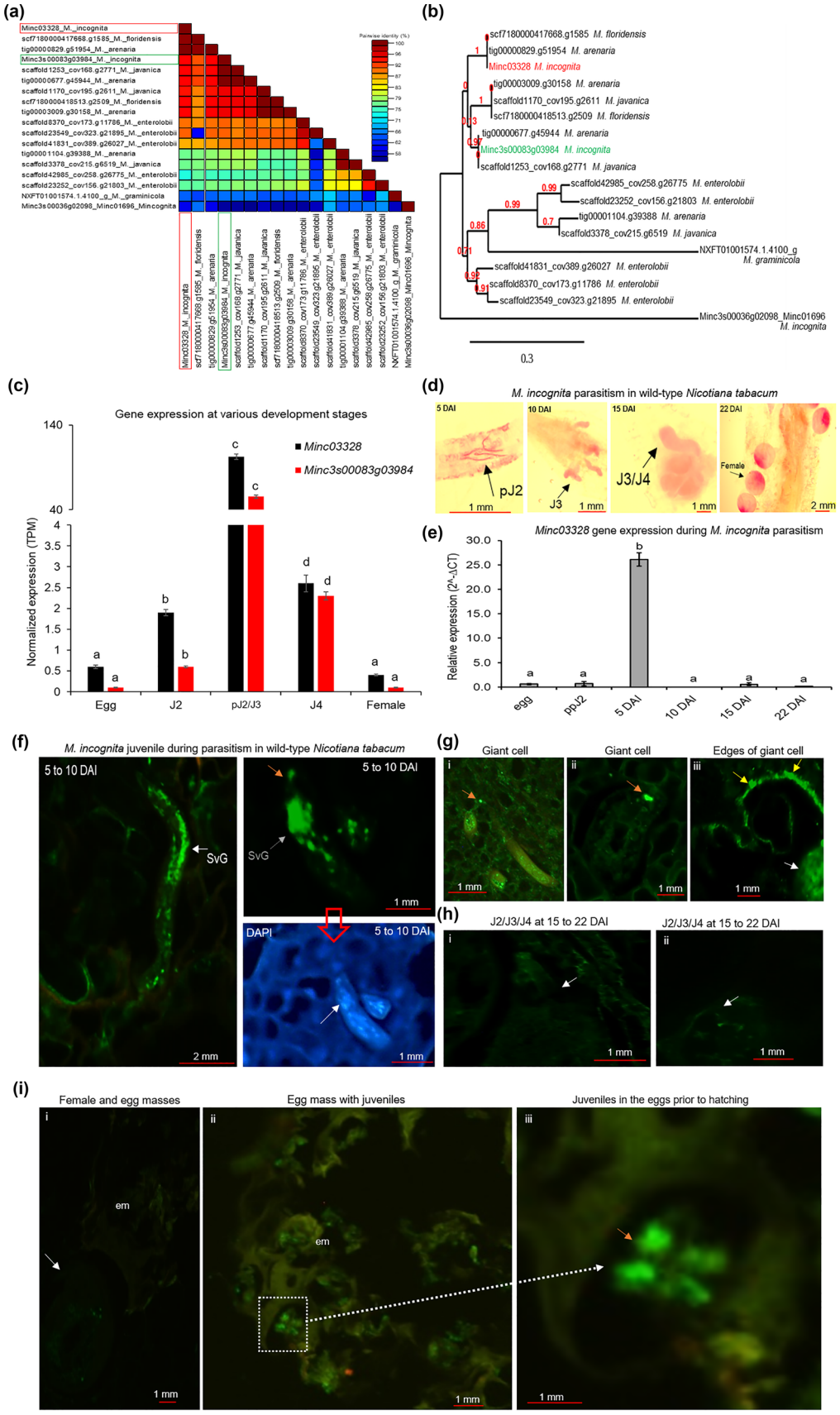
(a)
(b)
(c)
Gene expression at various development stages
Minc03328
Minc3s00083g03984
Normalized expression (TPM)
Egg
J2
pJ2/J3
J4
Female
(d)
M. incognita parasitism in wild-type Nicotiana tabacum
5 DAI
10 DAI
15 DAI
22 DAI
pJ2
J3
J3/J4
Female
(e)
Minc03328 gene expression during M. incognita parasitism
Relative expression (2^-ΔCT)
egg
ppJ2
5 DAI
10 DAI
15 DAI
22 DAI
(f)
M. incognita juvenile during parasitism in wild-type Nicotiana tabacum
5 to 10 DAI
SvG
DAPI
(g)
Giant cell
Giant cell
Edges of giant cell
(h)
J2/J3/J4 at 15 to 22 DAI
J2/J3/J4 at 15 to 22 DAI
(i)
Female and egg masses
Egg mass with juveniles
Juveniles in the eggs prior to hatching
em

◂**Fig. 1** In silico sequence analysis of the *M. incognita* effector genes, *Minc03328* effector gene expression, and Minc03328 effector protein immunolocalization in *M. incognita*. **a** Pairwise sequence identity matrices of nucleotide sequences generated using Sequence Demarcation Tool version 1.2 software. **b** Evolutionary analysis of nucleotide sequences generated by the Phylogeny.fr web service. Highlighted in red and green boxes or letters are, respectively, *Minc03328* gene studied in this work and its paralogue gene. The gene sequences were retrieved from WormBase Parasite Database version WBPS13. **c** *Minc03328* and *Minc3s00083g03984* gene expression profile in different *M. incognita* life stages: egg, pJ2, J3, J4, and female, from transcriptome datasets under BioProject number: PRJNA390559 (Choi et al. 2017), retrieved from BioSample database (NCBI). Error bars represent confidence intervals corresponding to three libraries per nematode life stage. **d** Histopathological images of *M. incognita* pJ2, J3, J3/J4, and female in *N. tabacum* roots stained with acid fuchsin at 5, 10, 15, and 22 days after inoculation (DAI). **e** *Minc03328* gene expression profile measured by real-time RT-qPCR analysis in different *M. incognita* race 3 life stages (egg, ppJ2, and pJ2 to female) during its parasitism in *N. tabacum*. Relative expression levels were normalized with *Mi18S* and *MiGAPDH* as endogenous reference genes (Suppl. Table S1). Error bars represent confidence intervals corresponding to three biological replicates. Different letters on bars indicate significant differences based on Tukey's test at 5% significance level. **f** Minc03328 effector protein immunolocalization in *M. incognita* pJ2 during its parasitism in wild-type *N. tabacum* plants. Minc03328 protein (bright green fluorescence signal) was localized in subventral glands (SvG) (white arrow) and at the head tip (orange arrow) of *M. incognita* pJ2s during its parasitism in *N. tabacum* roots at 5 to 10 DAI. **g** A significant fluorescence signal was observed in giant cells near the head tip of nematode (i and ii; indicate by orange arrows), while in some galls, a strong fluorescence signal was observed at the edges of giant cells (iii; yellow arrows); white arrow indicates the nematode. **h** No detected fluorescence signal was observed in J3/J4 at 15–22 DAI (i and ii; white arrows). **i** No detected fluorescence signal was observed in females (i; white arrow) and egg masses (ii; indicates by "em") at 22–45 DAI, but a powerful fluorescence signal was visible within juveniles (iii; orange arrow) in the eggs before hatching. The immunolocalization experiments were performed using a primary anti-Minc03328 antibody and a secondary anti-rabbit ALEXA-488-conjugated antibody. Fluorescence images represent longitudinal sections of a butyl-methyl methacrylate mixture embedded pJ2 during its parasitism in *N. tabacum*. Weak green color is autofluorescence of the fixed tissues

pots containing sterile substrate/sand mixture (1:1, *v*/*v*) and inoculated with *M. incognita* ppJ2s. At 5 DAI, the transgene and *Minc03328* effector gene expression were evaluated by RT-qPCR analysis. The RT-qPCR analysis revealed a high RNAi transgene expression level in *M. incognita*-infected galls of all four transgenic *A. thaliana* lines (Fig. 2d). Consistent with this, the *Minc03328* effector gene expression in *M. incognita* pJ2 to J3 fed on transgenic roots at 5 DAI was strongly decreased in all four transgenic lines compared to wild-type control plants (Fig. 2e). At 60 DAI, gall and egg mass number, and their ratio [gall/egg masses number] were assessed to estimate plant susceptibility to *M. incognita*. All four transgenic lines carrying the RNAi construct downregulating the *Minc03328* effector gene showed reduced susceptibility to *M. incognita* compared to wild-type control plants. The number of galls per plant was reduced up to 85% (Fig. 2f), egg masses were reduced up to 90% (Fig. 2g), and the [gall/egg masses number] ratio was reduced up to 87% (Fig. 2h) in transgenic lines. Collectively, these data confirmed that a reduced percentage of the *M. incognita* ppJ2s inoculated in these transgenic Minc03328-dsRNA lines successfully reached the final infection cycle. In accordance, the development and reproductive cycle of at least 64% of inoculated ppJ2s were disturbed by *in planta Minc03328* gene downregulation. Consistently with these previous data, [galls/egg masses number] ratio suggests that *Minc03328* effector gene downregulation significantly affected *M. incognita* parasitism in plants and delayed pJ2, J3, and J4 development in adult females, reflecting negatively on production of egg masses.

To investigate gall and nematode development during parasitism in plants, we analyzed gall morphology at 45 DAI from a selected transgenic line compared to wild type. Histopathological morphology analysis was focused only on Line #1, because it showed identical susceptibility levels to Minc03328-dsRNA Line #2, #3, and #4 (Fig. 2e–h). Wild-type *A. thaliana* roots showed clearly higher number and more prominent *M. incognita*-induced galls (Fig. 3a) compared with roots from transgenic *A. thaliana* line, which showed fewer and smaller galls (Fig. 3b). Interestingly, galls from wild-type control plants showed the presence of well-developed nematodes (Fig. 3c) compared with the delayed development of nematode in transgenic plants (Fig. 3d). In addition, galls from wild-type plants showed typical giant cells with high cytoplasmic content (Fig. 3c, e, and g), whereas galls induced in transgenic plants showed fewer cytoplasm content and presented cell-wall stubs suggesting attempted cell wall formation (Fig. 3d, f, and h). Neighboring cells from transgenic plants showed xylem, giant cells, and neighboring cells with irregular sizes and shapes suggesting altered gall ontogenesis (Fig. 3d and f; Suppl. Fig. S4) compared with galls and neighboring cells from wild type plants, which showed better cellular organization (Fig. 3c and e; Suppl. Fig. S4). Another notable feature was that nematodes in wild-type apparently developed faster and presented a more defined cuticle (Fig. 3c, e, and g), whereas a delayed nematode development was apparent in transgenic plants (Fig. 3d, f, and h; Suppl. Fig. S4). In addition, mature female cuticle during nematode parasitism in wild-type plants was well defined and perfectly visible (Fig. 3c, e, and g). In contrast, cuticle of nematodes in transgenic lines were not well defined and clearly disturbed presenting an undefined morphology and were weakly staining during nematode parasitism in Minc03328-dsRNA transgenic plants (Fig. 3d, f, and h; Suppl. Fig. S4). Thus, the gall morphology in transgenic *A. thaliana* illustrated the consequence of the *Minc03328* gene downregulation during *M. incognita* infection, feeding sites induction, and giant cell ontogenesis, leading to important deleterious effects on

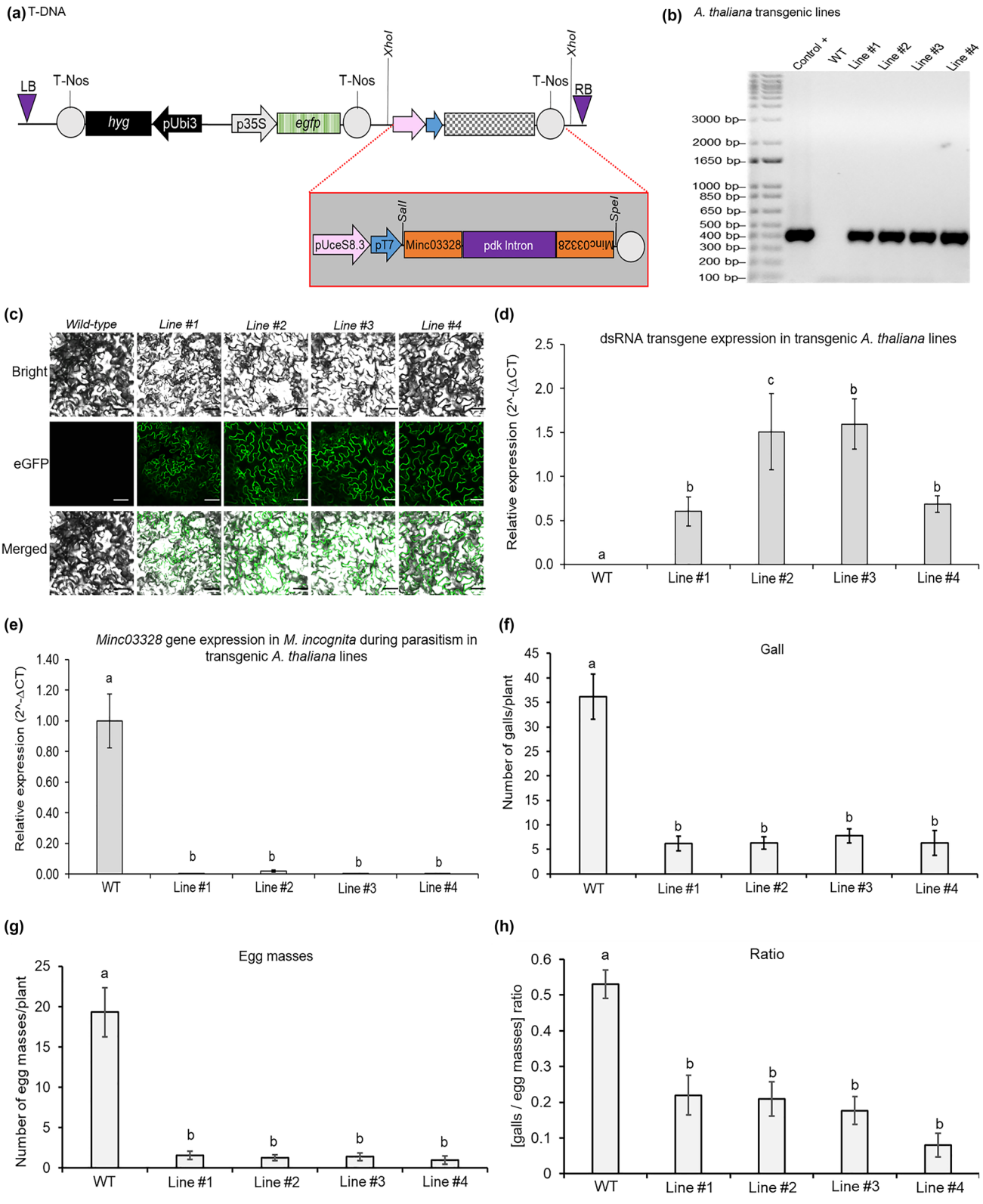
(a) T-DNA
LB
T-Nos
hyg
pUbi3
p35S
egfp
T-Nos
XhoI
T-Nos
XhoI
RB
SalI
SpeI
pUceS8.3
pT7
Minc03328
pdk Intron
Minc03328
(b) A. thaliana transgenic lines
Control +
WT
Line #1
Line #2
Line #3
Line #4
3000 bp
2000 bp
1650 bp
1000 bp
850 bp
650 bp
500 bp
400 bp
300 bp
200 bp
100 bp
(c)
Wild-type
Line #1
Line #2
Line #3
Line #4
Bright
eGFP
Merged
(d)
dsRNA transgene expression in transgenic A. thaliana lines
Relative expression (2^-(ΔCT))
WT
Line #1
Line #2
Line #3
Line #4
(e)
Minc03328 gene expression in M. incognita during parasitism in transgenic A. thaliana lines
Relative expression (2^-ΔCT)
(f)
Gall
Number of galls/plant
(g)
Egg masses
Number of egg masses/plant
(h)
Ratio
[galls / egg masses] ratio

◂**Fig. 2** *Agrobacterium*-mediated *A. thaliana* genetic transformation, dsRNA transgene expression in transgenic Minc03328-dsRNA lines, *Minc03328* effector gene expression in *M. incognita* during its parasitism in transgenic lines, and susceptibility level of transgenic *A. thaliana* lines for *M. incognita* race 3. **a** Overview of the vector-DNA used for genetic transformation of *A. thaliana* plants, targeting downregulation of the nematode *Minc03328* effector transcript by the *in planta* RNAi strategy. **b** PCR detection of the dsRNA transgene in *A. thaliana* lines indicating 400-bp expected size amplificon. Marker: 1.0-kb DNA ladder (Invitrogen, Cat. #10787018); Positive control: water-diluted binary vector; WT: non-transgenic line used as a negative control for PCR and bioassays. **c** Fluorescence detection of GFP protein in transgenic lines under a Zeiss inverted LSM510 META laser scanning microscope using 488-nm excitation line and the 500–530-nm band-pass filter (Carl Zeiss). Scale bars: 10 mm. **d** dsRNA transgene expression level in *M. incognita*-infected galls of transgenic *A. thaliana* lines. The relative expression was calculated with 2^-ΔCT formula using *AtActin 2*, *AtGAPDH*, and *AtEF1* as endogenous reference genes (Suppl. Table S1). Error bars represent confidence intervals corresponding to three biological replicates. Different letters on bars indicate statistically significant differences between transgenic Minc03328-dsRNA lines compared to wild-type control plants, according to Tukey's test at 5% significance level. **e** *Minc03328* gene expression in *M. incognita* during its parasitism in wild-type plants and transgenic lines. The relative expression was calculated with 2^-ΔCT formula using *MiGAPDH*, *MiActin,* and *Miβ-tubulin* as endogenous reference genes (Suppl. Table S1). Error bars represent confidence intervals corresponding to three biological replicates. Different letters on bars indicate statistically significant differences between *M. incognita* fed in transgenic lines compared to *M. incognita* fed in wild-type control plants, according to Tukey's test at 5% significance level. **f** Gall number per plant, **g** egg masses number per plant, and **h** [galls/egg masses] ratio in transgenic *A. thaliana* lines at 60 DAI. Error bars represent confidence intervals corresponding to 12–15 plants per line. Different letters on bars indicate statistically significant differences between transgenic lines compared to wild-type control plants, according to Tukey's test at 5% significance level

gall and nematode development. Therefore, considering that *Minc03328* gene expression is highest in early stages of *M. incognita* parasitism, our data suggest that *Minc03328* effector gene downregulation within nematodes during parasitism might negatively affect nematode infection, feeding site formation, gall genesis, and nematode development. Overall, our data strongly suggest the importance of *Minc03328* as an effector protein during *M. incognita* parasitism in host plants.

Discussion

Plant–parasitic nematodes are important phytopathogens that interfere in complex pathways of the plant hosts allowing the promotion of parasitism in numerous plant species (Quentin et al. 2013). In contrast, beyond preformed and basal defenses, higher plants exhibit another arsenal of pathogen-activated molecules (Vieira and Engler 2017; Sato et al. 2019; Cabral et al. 2020). First, root damage caused by nematode infection produces and accumulates

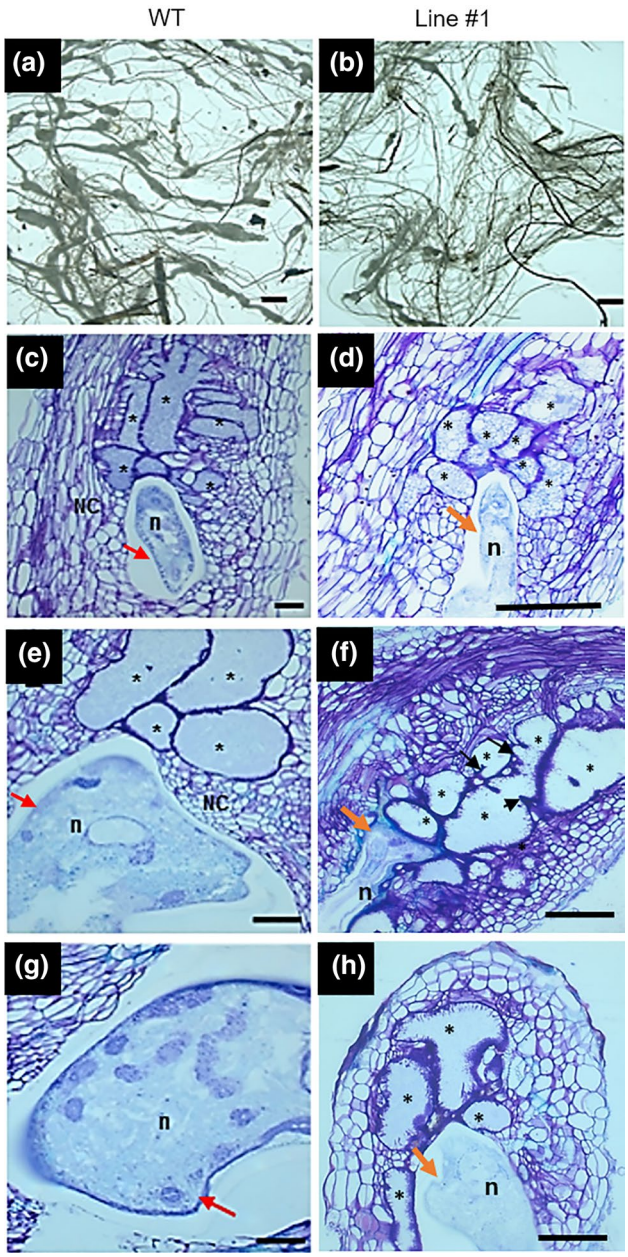

Fig. 3 Histopathological morphology of *M. incognita*-induced galls in transgenic Minc03328-dsRNA *A. thaliana* lines. Plants from transgenic Line #1 and wild-type control plants were submitted to *M. incognita* infection, and gall and nematode morphology were evaluated at 45 DAI. Sectioned galls were stained with toluidine blue. **a** and **b** Transgenic *A. thaliana* roots showed fewer and smaller galls compared to wild-type control plants. **c**–**f** Galls from wild-type control plants showed development of multiple feeding sites, giant cells filled with cytoplasm, and presented fastly maturing nematodes (identified by letter "n"). In contrast, galls from transgenic plants showed giant cells with a few cytoplasmic contents (identified by *) and often containing cell-wall stubs (black arrows). Similarly, galls and neighboring cells from transgenic lines showed a higher organization, while wild-type control plants showed xylem, galls, and neighboring cells with irregular sizes and shapes, suggesting altered giant cell ontogenesis. In the images **g**–**h**, the nematode cuticle was apparently disintegrated during *M. incognita* parasitism in transgenic *A. thaliana* plants compared to perfectly visible mature female cuticle during *M. incognita* parasitism in wild-type control plants (red arrows). This analysis demonstrated that *Minc03328* silencing caused a direct effect on nematode morphology as well indirectly in gall structure. Asterisks, giant cell; NC, neighboring cells; n, nematode. Scale bars = 50 µm

molecules that act *in trans* as damage-associated molecular patterns (DAMPs) that, consequently, activate pattern-triggered immunity (PTI). In addition, nematode-associated molecular patterns (NAMPs) enhance plant basal defense (NAMPs triggered immunity) (Ali et al. 2018). The second level of plant defense responses against nematodes is related to effector-triggered immunity (ETI) (Holbein et al. 2016). In contrast, PPNs secrete several effector proteins during host plant–nematode interaction to overcome these defense mechanisms and promote its parasitism in host plants (Vieira and Gleason 2019). More specifically, these nematode effector proteins act by disrupting the plant defense response and modulating the plant cell cycle and cellular development (Vieira and Gleason 2019). Interestingly, many nematode effectors interact with host plant proteins, individually or collectively suppressing host defense signaling or preventing PTI and ETI activation (Manosalva et al. 2015; Zhao et al. 2019; Mendes et al. 2021a, b). At the same time, other effectors can act by interacting and destabilizing host plant proteins involved in specific biological processes to make them suitable for nematode infection.

RKN (*Meloidogyne* spp.) are major crop pathogen worldwide, and limited range of available control agents or resistant/tolerant cultivars has significantly limited the effectiveness of its control and management (Seo and Kim 2014; Bernard et al. 2017). The low effectiveness of control measures in the field and the emergence of resistant or tolerant RKN populations have led to the use of genetically engineered cultivars to overcome these drawbacks. Following the sequencing and evaluation of the *M. incognita* genome (Abad et al. 2008; Blanc-Mathieu et al. 2017), several candidate effector proteins have been identified. However, the information about their biological functions after secretion in host plants or their action mode in plant cells is still poorly understood (Bellafiore et al. 2008; Lin et al. 2013; Rutter et al. 2014; Mejias et al. 2019).

In this study, the *Minc03328* gene and its effector protein were characterized and their involvement in *M. incognita* parasitism in plants was successfully confirmed. Sequence analysis showed the absence of cytoplasmic and transmembrane domains and the presence of a secretory signal peptide. In addition, orthologous or paralogous genes for *Minc03328* were also identified in other species from *Meloidogyne* sp. genus, suggesting that this effector pathway can be functionally conserved in other *Meloidogyne* species, mainly in *M. arenaria* and *M. floridensis*. In contrast, low sequence identity of *Minc03328* was observed with other already well-characterized effector genes, indicating that this particular effector might act in a specific pathway during parasitism. At the same time, its paralogue gene showed high sequence identity to *Minc03328*, being 93% (1342/1444) for nucleotide and 88% (424/481) for amino acid sequences. These observations based on sequence analysis suggest that both genes can act in a common particular effector pathway and might present redundant functions. The *Minc03328* gene expression analysis showed higher expression at onset of parasitism, and the immunocytochemical analysis proved that Minc03328 protein was accumulated in subventral glands and was observably secreted and possibly accumulated in giant cells. These collective data support that Minc03328 can be considered an effector protein closely involved during *M. incognita* parasitism in host plants. In addition, our data are in accordance with Rutter et al. (2014), which showed that *Minc03328* effector gene expression was upregulated in *M. incognita* at 3–14 DAI and showed that *Minc03328* transcript accumulated specifically in subventral glands.

Herein, we found that downregulation of this effector gene using *in planta* RNAi strategy in transgenic Minc03328-dsRNA *A. thaliana* lines consistently attenuated the parasitic capacity of *M. incognita*. Remarkably, overexpression of the dsRNA transgene in Arabidopsis lines caused a significant reduction in number of galls and egg masses, and [galls/egg masses] ratio compared with wild-type control plants. These data indicate that *Minc03328* can be in fact an effector gene with highlighted importance in plant parasitism by *M. incognita*. Since dsRNA sequence used as RNAi in this study can target both *Minc03328* and its paralogue gene, these phenotypic data, which reduced plant susceptibility to nematodes observed in the transgenic plants, indicate that this effector pathway, which could be controlled by the effector Minc03328 itself, and possibly also by its paralogue gene, might be significantly affected or compromised in some way.

Morphological analyses of *M. incognita*-induced galls showed that pJ2s fed on Minc03328 downregulated lines struggle to induce and establish feeding sites, and inhibit the progression of gall development. Since *Minc03328* effector gene expression was upregulated at 5 DAI in J2/J3s, these morphological analyses supported that its knockdown somehow strongly impaired giant cells metabolic activity and development. Giant cells displayed few cytoplasm contents and cell-wall stubs added to the observation that nematode cuticle appears to lose its structure likely hampering nematode parasitism in transgenic plants. These morphological results fully support that *Minc03328*-dsRNA overexpression downregulates *Minc03328* gene activity reducing plant susceptibility to nematodes.

Similar to previous results with other effectors, the knockdown of a single effector gene can be sufficient to impair nematode parasitism (unpublished data). Thus, data obtained in this present study collectively confirm that the *Minc03328* gene acts as a potent effector protein important for the successful parasitism of *M. incognita* in host plants. It was once again demonstrated that *in planta* RNAi

strategy is highly effective in downregulating *M. incognita* effector genes. To date, several *M. incognita* effector genes or other nematode genes have been characterized and validated using *in planta* RNAi strategy (Suppl. Table S3) (Basso et al. 2020). Similarly, the downregulation of any of the three effector genes *Minc01696*, *Minc00344*, and *Minc00801* was shown to be sufficient to strongly disturb *M. incognita* parasitism in plants (unpublished data). Data presented here, together with those in the literature, have shown that although *M. incognita* has dozens of effector proteins acting in the modulation of its parasitism in plants, the disruption of one or some of these genes can significantly compromise the infectious process of the nematode (Mejias et al. 2019; Mendes et al. 2021a, b). Thus, using *in planta* RNAi strategy to downregulate *Minc03328* effector gene in economically important crops such as cotton and soybean is an interesting biotechnological approach to decrease plant susceptibility to *M. incognita*. Recently, Lisei-de-Sa et al. (2021), using a similar strategy, showed that triple downregulation of *cysteine protease*, *isocitrate lyase*, and *splicing factor* genes significantly impaired *M. incognita* parasitism in transgenic cotton lines. Understanding the action mode of this effector when secreted in plant cells will provide further evidence in the plant–nematode interaction. Previous studies reported by Mukhtar et al. (2011), Consortium (2011), and Wessling et al. (2014) showed that different and diverse pathogen effectors could target the same hub protein of the host plant during its parasitism.

In conclusion, we have here explored the *Minc03328* gene function during parasitism, confirming that Minc03328 protein acts as a powerful effector of substantial importance for successful *M. incognita* parasitism in plants. Since the dsRNA sequence used in this study possibly downregulated not only *Minc03328* but also its paralogue *Minc3s00083g03984* gene, the complete disruption of this effector pathway likely contributed to the reduced susceptibility observed in transgenic Minc03328-dsRNA lines. Finally, our findings demonstrated that the *Minc03328* effector gene and, possibly, its paralogue gene could be powerful targets for biotechnological approaches like *in planta* RNAi technology for *M. incognita* control and management in economically important crops.

Author contribution statement MFGS was the major investigator on this project. MFGS, ITLT, and VJVM designed all experiments. VJVM, FBMA, and DMS performed PCR experiments, plant generation advancements, bioassays, and fuchsin staining, and wrote first draft of the manuscript. MFB performed sequence analyses, produced transgenic *A. thaliana* lines and, helped by MFGS, elaborated final version of the manuscript. MELS provided *M. incognita* inoculum and assisted with bioassays. ITLT and JAE carried out Minc03328 protein immunolocalization and performed *M. incognita*-infected galls histological examination. VJVM, ITLT, and BPM performed real-time RT-qPCR analysis. CVM held with statistical analysis. MFGS, MCMS, and JAE analyzed data, provided intellectual inputs, and amended the manuscript. All authors read and approved the final version of the manuscript.

Supplementary Information The online version contains supplementary material available at https://doi.org/10.1007/s00425-022-03823-4.

Acknowledgements The authors are grateful to EMBRAPA, UCB, CNPq, INCT PlantStress Biotech, CAPES, and FAP-DF for the scientific and financial support.

Funding This work was supported by grants from INCT PlantStress Biotech, UCB, CNPq, CAPES, FAP-DF, INRAE, and EMBRAPA. MFB is grateful to CNPq for a postdoctoral research fellowship (PDJ 150936/2018-4). MFGS is grateful to CAPES/Cofecub project for financial support in the researcher and students' exchange program between institutions.

Declarations

Conflict of interest The authors declare no conflict of interest.

References

Abad P, Gouzy J, Aury J-M, Castagnone-Sereno P et al (2008) Genome sequence of the metazoan plant-parasitic nematode *Meloidogyne incognita*. Nature Biotechnol 26:909. https://doi.org/10.1038/nbt.1482

Ali MA, Anjam MS, Nawaz MA, Lam H-M, Chung G (2018) Signal transduction in plant-nematode interactions. Intern J Mol Sci 19(6):1648. https://doi.org/10.3390/ijms19061648

Basso MF, Lourenço-Tessutti IT, Mendes RAG, Pinto CEM, Bournaud C, Gillet F-X, Togawa RC, de Macedo LLP, de Almeida EJ, Grossi-de-Sa MF (2020) *MiDaf16-like* and *MiSkn1-like* gene families are reliable targets to develop biotechnological tools for the control and management of *Meloidogyne incognita*. Sci Rep 10(1):6991. https://doi.org/10.1038/s41598-020-63968-8

Bellafiore S, Shen Z, Rosso MN, Abad P, Shih P, Briggs SP (2008) Direct identification of the *Meloidogyne incognita* secretome reveals proteins with host cell reprogramming potential. PLoS Pathog 4(10):e1000192. https://doi.org/10.1371/journal.ppat.1000192

Bernard GC, Egnin M, Bonsi C (2017) The impact of plant-parasitic nematodes on agriculture and methods of control. In: Shah MM, Mahamood M (eds) Nematology-concepts, diagnosis and control. Intech, London. https://doi.org/10.5772/intechopen.68958

Blanc-Mathieu R, Perfus-Barbeoch L, Aury J-M, Da Rocha M, Gouzy J, Sallet E, Martin-Jimenez C, Bailly-Bechet M, Castagnone-Sereno P, Flot J-F, Kozlowski DK, Cazareth J, Couloux A, Da Silva C, Guy J, Kim-Jo Y-J, Rancurel C, Schiex T, Abad P, Wincker P, Danchin EGJ (2017) Hybridization and polyploidy enable genomic plasticity without sex in the most devastating plant-parasitic nematodes. PLoS Genet 13(6):e1006777. https://doi.org/10.1371/journal.pgen.1006777

Blum M, Chang H-Y, Chuguransky S, Grego T, Kandasaamy S et al (2020) The InterPro protein families and domains database: 20

years on. Nucleic Acids Res 49(D1):D344–D354. https://doi.org/10.1093/nar/gkaa977
Bolger AM, Lohse M, Usadel B (2014) Trimmomatic: a flexible trimmer for Illumina sequence data. Bioinformatics 30(15):2114–2120. https://doi.org/10.1093/bioinformatics/btu170
Bournaud C, Gillet F-X, Murad AM, Bresso E, Albuquerque EVS, Grossi-de-Sa MF (2018) *Meloidogyne incognita PASSE-MURAILLE* (*MiPM*) gene encodes a cell-penetrating protein that interacts with the CSN5 subunit of the COP9 signalosome. Front Plant Sci 9:904. https://doi.org/10.3389/fpls.2018.00904
Bray NL, Pimentel H, Melsted P, Pachter L (2016) Near-optimal probabilistic RNA-seq quantification. Nat Biotechnol 34(5):525–527. https://doi.org/10.1038/nbt.3519
Bybd DW, Kirkpatrick T, Barker KR (1983) An improved technique for clearing and staining plant tissues for detection of nematodes. J Nematol 15(1):142–143
Cabral D, Banora MY, Antonino JD, Rodiuc N, Vieira P, Coelho RR, Chevalier C, Eekhout T, Engler G, De Veylder L, Grossi-de-Sa MF, de Almeida EJ (2020) The plant WEE1 kinase is involved in checkpoint control activation in nematode-induced galls. New Phytol 225(1):430–447. https://doi.org/10.1111/nph.16185
Canteri MG, Althaus RA, Virgens Filho JS, Giglioti EA, Godoy CV (2001) SASM-Agri : sistema para análise e separação de médias em experimentos agrícolas pelos métodos Scoft-Knott, Tukey e Duncan. Rev Bras De Agrocomputação 1(2):18–24
Carneiro RG, Mazzafera P, Ferraz LCCB, Muraoka T, Trivelin PCO (2002) Uptake and translocation of nitrogen, phosphorus and calcium in soybean infected with *Meloidogyne incognita* and *M. javanica*. Fitopatol Bras 27:141–150
Castagnone-Sereno P, Danchin EGJ, Perfus-Barbeoch L, Abad P (2013) Diversity and evolution of root-knot nematodes, genus *Meloidogyne*: new insights from the genomic Era. Annu Rev Phytopathol 51(1):203–220. https://doi.org/10.1146/annurev-phyto-082712-102300
Choi I, Subramanian P, Shim D, Oh B-J, Hahn B-S (2017) RNA-Seq of plant-parasitic nematode *Meloidogyne incognita* at various stages of its development. Front Genet 8:190–190. https://doi.org/10.3389/fgene.2017.00190
Clough SJ, Bent AF (1998) Floral dip: a simplified method for *Agrobacterium*-mediated transformation of *Arabidopsis thaliana*. Plant J 16(6):735–743. https://doi.org/10.1046/j.1365-313x.1998.00343.x
Consortium AIM (2011) Evidence for network evolution in an *Arabidopsis* interactome map. Science 333(6042):601–607. https://doi.org/10.1126/science.1203877
de Engler EJ, Kyndt T, Vieira P, Van Cappelle E, Boudolf V, Sanchez V, Escobar C, De Veylder L, Engler G, Abad P, Gheysen G (2012) *CCS52* and *DEL1* genes are key components of the endocycle in nematode-induced feeding sites. Plant J 72(2):185–198. https://doi.org/10.1111/j.1365-313X.2012.05054.x
Doyle JJ, Doyle JL (1987) A rapid DNA isolation procedure for small quantities of fresh leaf tissue. Phytochem Bull 19:11–15
El-Gebali S, Mistry J, Bateman A, Eddy SR, Luciani A, Potter SC, Qureshi M, Richardson LJ, Salazar GA, Smart A, EL Sonnhammer L, Hirsh L, Paladin L, Piovesan D, Tosatto SCE, Finn RD (2018) The Pfam protein families database in 2019. Nucleic Acids Res 47(D1):D427–D432. https://doi.org/10.1093/nar/gky995
Grossi-de-Sa MF, Guimaraes LM, Batista JAN, Viana AAB, da Rocha Fragoso R, da Silva MCM (2013) Compositions and methods for modifying gene expression using the promoter of ubiquitin conjugating protein coding gene of soybean plants. Patent US-201313770867-A
Grossi-de-Sa M, Petitot A-S, Xavier DA, Sá MEL, Mezzalira I, Beneventi MA, Martins NF, Baimey HK, Albuquerque EVS, Grossi-de-Sa MF, Fernandez D (2019) Rice susceptibility to root-knot nematodes is enhanced by the *Meloidogyne incognita MSP18* effector gene. Planta 250(4):1215–1227. https://doi.org/10.1007/s00425-019-03205-3
Harrison SJ, Mott EK, Parsley K, Aspinall S, Gray JC, Cottage A (2006) A rapid and robust method of identifying transformed *Arabidopsis thaliana* seedlings following floral dip transformation. Plant Method 2(1):19. https://doi.org/10.1186/1746-4811-2-19
Holbein J, Grundler FMW, Siddique S (2016) Plant basal resistance to nematodes: an update. J Exp Bot 67(7):2049–2061. https://doi.org/10.1093/jxb/erw005
Huang G, Gao B, Maier T, Allen R, Davis EL, Baum TJ, Hussey RS (2003) A profile of putative parasitism genes expressed in the esophageal gland cells of the root-knot nematode *Meloidogyne incognita*. Mol Plant-Microbe Interact 16(5):376–381. https://doi.org/10.1094/mpmi.2003.16.5.376
Hussey RS, Barker KR (1973) A comparison of methods of collecting inocula of *Meloidogyne* spp., including a new technique. Plant Dis Rep 57:1025–1028
Kronenberger J, Desprez T, Höfte H, Caboche M, Traas J (1993) A methacrylate embedding procedure developed for immunolocalization on plant tissues is also compatible with in situ hybridization. J Histochem Cytochem 17(11):1013–1021. https://doi.org/10.1006/cbir.1993.1031
la Cour T, Kiemer L, Molgaard A, Gupta R, Skriver K, Brunak S (2004) Analysis and prediction of leucine-rich nuclear export signals. Protein Eng Des Sel 17(6):527–536. https://doi.org/10.1093/protein/gzh062
Lee RYN, Howe KL, Harris TW, Arnaboldi V, Cain S et al (2017) WormBase 2017: molting into a new stage. Nucleic Acids Res 46(D1):D869–D874. https://doi.org/10.1093/nar/gkx998
Lin B, Zhuo K, Wu P, Cui R, Zhang L-H, Liao J (2013) A novel effector protein, Mj-NULG1a, targeted to giant cell nuclei plays a role in *Meloidogyne javanica* parasitism. Mol Plant-Microbe Interact 26(1):55–66. https://doi.org/10.1094/mpmi-05-12-0114-fi
Lisei-de-Sá ME, Rodrigues-Silva PL, Morgante CV, de Melo BP, Lourenço-Tessutti IT, Arraes FBM, Sousa JPA, Galbieri R, Amorim RMS, de Lins CBJ, Macedo LLP, Moreira VJ, Ferreira GF, Ribeiro TP, Fragoso RR, Silva MCM, de Almeida-Engler J, Grossi-de-Sa MF (2021) Pyramiding dsRNAs increases phytonematode tolerance in cotton plants. Planta 254(6):121. https://doi.org/10.1007/s00425-021-03776-0
Lu P, Davis RF, Kemerait RC, van Iersel MW, Scherm H (2014) Physiological effects of *Meloidogyne incognita* infection on cotton genotypes with differing levels of resistance in the greenhouse. J Nematol 46(4):352–359
Manosalva P, Manohar M, von Reuss SH, Chen S, Koch A, Kaplan F, Choe A, Micikas RJ, Wang X, Kogel K-H, Sternberg PW, Williamson VM, Schroeder FC, Klessig DF (2015) Conserved nematode signalling molecules elicit plant defenses and pathogen resistance. Nature Commun 6:7795. https://doi.org/10.1038/ncomms8795
Marchler-Bauer A, Derbyshire MK, Gonzales NR, Lu S, Chitsaz F, Geer LY, Geer RC, He J, Gwadz M, Hurwitz DI, Lanczycki CJ, Lu F, Marchler GH, Song JS, Thanki N, Wang Z, Yamashita RA, Zhang D, Zheng C, Bryant SH (2015) CDD: NCBI's conserved domain database. Nucleic Acids Res 43(Database issue):222–226. https://doi.org/10.1093/nar/gku1221
Mejias J, Truong NM, Abad P, Favery B, Quentin M (2019) Plant proteins and processes targeted by parasitic nematode effectors. Front Plant Sci 10:970. https://doi.org/10.3389/fpls.2019.00970
Melakeberhan H, Webster JM, Brooke RC, D'Auria JM, Cackette M (1987) Effect of *Meloidogyne incognita* on plant nutrient concentration and its influence on the physiology of beans. J Nematol 19(3):324–330
Mendes RA, Basso MF, Fernandes de Araújo J, Paes de Melo B, Lima RN, Ribeiro TP, da Silva MV, Saliba Albuquerque EV,

Grossi-de-Sa M, Dessaune Tameirao SN, da Rocha FR, Mattar da Silva MC, Vignols F, Fernandez D, Grossi-de-Sa MF (2021a) Minc00344 and Mj-NULG1a effectors interact with GmHub10 protein to promote the soybean parasitism by *Meloidogyne incognita* and *M. javanica*. Exp Parasitol 229:108153. https://doi.org/10.1016/j.exppara.2021.108153

Mendes RA, Basso MF, Paes de Melo B, Ribeiro TP, Lima RN, Fernandes de Araújo J, Grossi-de-Sa M, da Silva MV, Togawa RC, Saliba Albuquerque ÉV, Lisei-de-Sa ME, Mattar da Silva MC, Pepino Macedo LL, da Rocha FR, Fernandez D, Vignols F, Grossi-de-Sa MF (2021b) The Mi-EFF1/Minc17998 effector interacts with the soybean GmHub6 protein to promote host–plant parasitism by *Meloidogyne incognita*. Physiol Mol Plant Pathol 114:101630. https://doi.org/10.1016/j.pmpp.2021.101630

Mukhtar MS, Carvunis AR, Dreze M, Epple P, Steinbrenner J, Moore J, Tasan M, Galli M, Hao T, Nishimura MT, Pevzner SJ, Donovan SE, Ghamsari L, Santhanam B, Romero V, Poulin MM, Gebreab F, Gutierrez BJ, Tam S, Monachello D, Boxem M, Harbort CJ, McDonald N, Gai L, Chen H, He Y, Vandenhaute J, Roth FP, Hill DE, Ecker JR, Vidal M, Beynon J, Braun P, Dangl JL (2011) Independently evolved virulence effectors converge onto hubs in a plant immune system network. Science 333(6042):596–601. https://doi.org/10.1126/science.1203659

Nguyen CN, Perfus-Barbeoch L, Quentin M, Zhao J, Magliano M, Marteu N, Da Rocha M, Nottet N, Abad P, Favery B (2018) A root-knot nematode small glycine and cysteine-rich secreted effector, MiSGCR1, is involved in plant parasitism. New Phytol 217(2):687–699. https://doi.org/10.1111/nph.14837

Nguyen Ba AN, Pogoutse A, Provart N, Moses AM (2009) NLStradamus: a simple Hidden Markov Model for nuclear localization signal prediction. BMC Bioinform 10:202. https://doi.org/10.1186/1471-2105-10-202

Orfanoudaki G, Markaki M, Chatzi K, Tsamardinos I, Economou A (2017) MatureP: prediction of secreted proteins with exclusive information from their mature regions. Sci Rep 7(1):3263. https://doi.org/10.1038/s41598-017-03557-4

Quentin M, Abad P, Favery B (2013) Plant parasitic nematode effectors target host defense and nuclear functions to establish feeding cells. Front Plant Sci 4:53. https://doi.org/10.3389/fpls.2013.00053

Rutter WB, Hewezi T, Abubucker S, Maier TR, Huang G, Mitreva M, Hussey RS, Baum TJ (2014) Mining novel effector proteins from the esophageal gland cells of *Meloidogyne incognita*. Mol Plant-Microbe Interact 27(9):965–974. https://doi.org/10.1094/mpmi-03-14-0076-r

Sato K, Kadota Y, Shirasu K (2019) Plant immune responses to parasitic nematodes. Front Plant Sci 10:1165. https://doi.org/10.3389/fpls.2019.01165

Schmittgen TD, Livak KJ (2008) Analyzing real-time PCR data by the comparative CT method. Nature Protoc 3:1101. https://doi.org/10.1038/nprot.2008.73

Seo Y, Kim YH (2014) Control of *Meloidogyne incognita* using mixtures of organic acids. Plant Pathol J 30(4):450–455. https://doi.org/10.5423/PPJ.NT.07.2014.0062

Shukla N, Yadav R, Kaur P, Rasmussen S, Goel S, Agarwal M, Jagannath A, Gupta R, Kumar A (2018) Transcriptome analysis of root-knot nematode (*Meloidogyne incognita*)-infected tomato (*Solanum lycopersicum*) roots reveals complex gene expression profiles and metabolic networks of both host and nematode during susceptible and resistance responses. Mol Plant Pathol 19(3):615–633. https://doi.org/10.1111/mpp.12547

St-Pierre J, Grégoire J-C, Vaillancourt C (2017) A simple method to assess group difference in RT-qPCR reference gene selection using GeNorm: the case of the placental sex. Sci Rep 7(1):16923. https://doi.org/10.1038/s41598-017-16916-y

Szitenberg A, Salazar-Jaramillo L, Blok VC, Laetsch DR, Joseph S, Williamson VM, Blaxter ML, Lunt DH (2017) Comparative genomics of apomictic root-knot nematodes: hybridization, ploidy, and dynamic genome change. Genome Biol Evol 9(10):2844–2861. https://doi.org/10.1093/gbe/evx201

Triantaphyllou A, Hirschmann H (1960) Post infection development of *Meloidogyne incognita* Chitwood 1949 (Nematoda-Heteroderidae). Ann De L'institut Phytopathologique Benaki 1:1–11

Trudgill DL, Blok VC (2001) Apomictic, polyphagous root-knot nematodes: exceptionally successful and damaging biotrophic root pathogens. Annu Rev Phytopathol 39:53–77. https://doi.org/10.1146/annurev.phyto.39.1.53

Truong NM, Chen Y, Mejias J, Soulé S, Mulet K, Jaouannet M, Jaubert-Possamai S, Sawa S, Abad P, Favery B, Quentin M (2021) The *Meloidogyne incognita* nuclear effector MiEFF1 interacts with arabidopsis cytosolic glyceraldehyde-3-phosphate dehydrogenases to promote parasitism. Front Plant Sci 12:633. https://doi.org/10.3389/fpls.2021.641480

Vieira P, de Engler A (2017) Plant cyclin-dependent kinase inhibitors of the KRP family: Potent inhibitors of root-knot nematode feeding sites in plant roots. Front Plant Sci 8:1514. https://doi.org/10.3389/fpls.2017.01514

Vieira P, Gleason C (2019) Plant–parasitic nematode effectors; insights into their diversity and new tools for their identification. Curr Opin Plant Biol 50:37–43. https://doi.org/10.1016/j.pbi.2019.02.007

Vieira P, Engler G, de Almeida EJ (2012) Whole-mount confocal imaging of nuclei in giant feeding cells induced by root-knot nematodes in Arabidopsis. New Phytol 195(2):488–496. https://doi.org/10.1111/j.1469-8137.2012.04175.x

Vilella AJ, Severin J, Ureta-Vidal A, Heng L, Durbin R, Birney E (2009) Ensembl Compara GeneTrees: complete, duplication-aware phylogenetic trees in vertebrates. Genome Res 19(2):327–335. https://doi.org/10.1101/gr.073585.107

Wessling R, Epple P, Altmann S, He Y, Yang L, Henz SR, McDonald N, Wiley K, Bader KC, Glasser C, Mukhtar MS, Haigis S, Ghamsari L, Stephens AE, Ecker JR, Vidal M, Jones JD, Mayer KF, Loren V, van Themaat E, Weigel D, Schulze-Lefert P, Dangl JL, Panstruga R, Braun P (2014) Convergent targeting of a common host protein-network by pathogen effectors from three kingdoms of life. Cell Host Microbe 16(3):364–375. https://doi.org/10.1016/j.chom.2014.08.004

Zhao J, Li L, Liu Q, Liu P, Li S, Yang D, Chen Y, Pagnotta S, Favery B, Abad P, Jian H (2019) A MIF-like effector suppresses plant immunity and facilitates nematode parasitism by interacting with plant annexins. J Exp Bot 70(20):5943–5958. https://doi.org/10.1093/jxb/erz348

Authors and Affiliations

Valdeir Junio Vaz Moreira[1,2,3] · Isabela Tristan Lourenço-Tessutti[1,4] · Marcos Fernando Basso[1,4] · Maria Eugênia Lisei-de-Sa[1,3,5] · Carolina Vianna Morgante[1,4,6] · Bruno Paes-de-Melo[1,7] · Fabrício Barbosa Monteiro Arraes[1,2,4] · Diogo Martins-de-Sa[1,3] · Maria Cristina Mattar Silva[1,4] · Janice de Almeida Engler[4,8] · Maria Fatima Grossi-de-Sa[1,4,9]

1 Embrapa Genetic Resources and Biotechnology, Brasilia, DF 70770-917, Brazil

2 Biotechnology Center, PPGBCM, UFRGS, Porto Alegre, RS 90040-060, Brazil

3 Federal University of Brasilia, UNB, Brasilia, DF 70910-900, Brazil

4 National Institute of Science and Technology, INCT PlantStress Biotech, Embrapa 70297-400, Brazil

5 Agriculture Research Company of Minas Gerais State, Uberaba, MG 31170-495, Brazil

6 Embrapa Semiarid, Petrolina, PE 56302-970, Brazil

7 Federal University of Viçosa, Viçosa, MG 36570-900, Brazil

8 INRAE, Université Côte d'Azur, CNRS, ISA, 06903 Sophia Antipolis, France

9 Catholic University of Brasilia, Brasilia, DF 71966-700, Brazil